# Multiomic Predictors of Short-Term Weight Loss and Clinical Outcomes During a Behavioral-Based Weight Loss Intervention

Janet C. Siebert [1], Maggie A. Stanislawski[1], Adnin Zaman[1], Danielle M. Ostendorf[1], Iain R. Konigsberg[1], Purevsuren Jambal[2], Diana Ir[1], Kristen Bing[1], Liza Wayland[1], Jared J. Scorsone[1], Catherine A. Lozupone[1], Carsten Görg[3], Daniel N. Frank[1], Daniel Bessesen[1], Paul S. MacLean[1], Edward L. Melanson [1,4,5], Victoria A. Catenacci [1]*, and Sarah J. Borengasser[2]*

**Objective:** Identifying predictors of weight loss and clinical outcomes may increase understanding of individual variability in weight loss response. We hypothesized that baseline multiomic features, including DNA methylation (DNAme), metabolomics, and gut microbiome, would be predictive of short-term changes in body weight and other clinical outcomes within a comprehensive weight loss intervention.

**Methods:** Healthy adults with overweight or obesity ($n = 62$, age 18-55 years, BMI 27-45 kg/m$^2$, 75.8% female) participated in a 1-year behavioral weight loss intervention. To identify baseline omic predictors of changes in clinical outcomes at 3 and 6 months, whole-blood DNAme, plasma metabolites, and gut microbial genera were analyzed.

**Results:** A network of multiomic relationships informed predictive models for 10 clinical outcomes (body weight, waist circumference, fat mass, hemoglobin A$_{1c}$, homeostatic model assessment of insulin resistance, total cholesterol, triglycerides, C-reactive protein, leptin, and ghrelin) that changed significantly ($P < 0.05$). For eight of these, adjusted $R^2$ ranged from 0.34 to 0.78. Our models identified specific DNAme sites, gut microbes, and metabolites that were predictive of variability in weight loss, waist circumference, and circulating triglycerides and that are biologically relevant to obesity and metabolic pathways.

**Conclusions:** These data support the feasibility of using baseline multiomic features to provide insight for precision nutrition–based weight loss interventions.

*Obesity* (2021) **29**, 859-869.

## Study Importance

### What is already known?

► High interindividual variability in weight loss response is a critical barrier to altering the current obesity epidemic.

► The gut microbiome, DNA methylation, and metabolomics are unique to each individual and are associated with obesity, weight loss, and phenotypic variability.

### What does this study add?

► For 8 of 10 clinical outcomes, including weight loss, statistically significant predictive models identified baseline multiomic predictors with robust effect sizes.

► Multiomic predictors were associated with known targets or pathways with biological relevance to obesity and weight loss.

### How might these results change the direction of research or the focus of clinical practice?

► These predictors can aid in generating specific hypotheses regarding metabolic pathways such as lipid metabolism, insulin signaling, and substrate use.

► The predictor networks provide evidence that the gut microbiome, epigenome, and metabolome interact with each other in a concerted manner.

► Using baseline multiomic predictors for weight loss response is feasible and may inform future behavioral weight loss interventions applying precision nutrition approaches.

## Introduction

Despite significant efforts to address the increasing prevalence of overweight and obesity, rates have continued to climb over the past two decades (1). Obesity has multiple etiologies and it is associated with a range of adverse health consequences, including cardiovascular disease (2,3). Current behavioral-based weight loss interventions typically produce on average only modest (~5%-10%) weight loss (4,5). However, focusing on this mean response

conceals the marked interindividual variability, with some individuals losing a substantial amount of weight and others losing no weight or even gaining weight during behavioral weight loss interventions (6). Variability of weight loss outcome is an important problem in the treatment of obesity, and understanding the factors underlying this variability may provide clues to more effectively tailor treatments for patients with precision nutrition approaches as described by others (7,8).

Contributors to interindividual variability in both weight loss and associated metabolic responses include genetics, epigenetics, gut microbiome (GM), and metabolomics (9,10). These inputs offer valuable molecular information, potentially serving as biomarkers of obesity, weight loss response, and heterogeneity in clinical outcomes. Demonstrating the predictive value of these molecular features is a first step toward identifying subphenotypes, which are small groups of individuals with similar baseline characteristics that vary in their response to intervention (11). By considering underlying biological systems, future behavioral weight loss programs can move away from a "one size (one intervention) fits all" approach.

The purpose of this study is to identify baseline multiomic predictors of weight loss and clinical outcomes within an ongoing, behavioral-based weight loss trial (the "parent trial"), a prospective randomized trial comparing weight loss generated by daily caloric restriction (DCR) versus intermittent fasting (IMF). Because the parent trial is ongoing, we do not report between-group differences. We hypothesized that baseline omic features, including DNA methylation (DNAme), GM, and circulating metabolites, could predict short-term weight loss and clinical outcomes. We created predictive models for 10 clinical outcomes showing a significant change from baseline, and we present details of the models for weight, waist circumference (WC), and triglycerides (TG). We selected these models for discussion because (1) change in weight is the primary outcome of the parent trial, and (2) among the other outcomes, the models for WC and TG represent the range of model complexity.

## Methods

### Participants and weight loss intervention

We conducted an ancillary study that included healthy men and women with overweight or obesity (age 18-55 years, BMI 27-45 kg/m$^2$) participating in an ongoing, two-arm randomized trial (ClinicalTrials.gov NCT03411356) comparing weight loss generated by DCR versus IMF. All participants received a 12-month guidelines-based, comprehensive, behavioral weight loss intervention consisting of an energy-restricted diet, increased physical activity, and group-based behavioral support. Participants in both randomized groups targeted an identical weekly dietary energy deficit (34%) from estimated individual weight maintenance energy requirements and differed only in the dietary strategy used to achieve this energy deficit. The DCR group targeted a 34% daily energy deficit, whereas the IMF group targeted an 80% energy deficit on three nonconsecutive "fast" days a week and were instructed to eat their usual baseline weight maintenance diet on fed days. We used biospecimens and clinical outcomes collected at baseline, 3 months, and 6 months in $n = 62$ participants in both arms of the first two cohorts of the parent study (DCR = 27, IMF = 35) enrolled in 2018-2019 (CONSORT diagram in Supporting Information, section 1.1.2). This study was approved by the University of Colorado Multiple Institutional Review Board. Participants provided informed consent in accordance with the principles described in the Declaration of Helsinki of 1975, revised in 1983. Additional details regarding the parent trial, including inclusion/exclusion criteria and a detailed description of study procedures and clinical outcomes, are provided in the Supporting Information.

### Clinical outcomes

Measurements of clinical outcomes, including weight, BMI, WC, systolic blood pressure (SBP), diastolic blood pressure, and body composition (dual energy X-ray absorptiometry), were conducted by trained study personnel. Methods are detailed in Supporting Information.

### Biospecimens

Twelve-hour fasting whole-blood samples were processed for plasma or immediately frozen and stored at −80°C. Plasma was assessed for glucose, insulin, total cholesterol (T. Chol), high-density lipoprotein cholesterol, low-density lipoprotein cholesterol, TG, leptin, ghrelin, peptide YY, hemoglobin A$_{1c}$, and C-reactive protein (CRP). Plasma betaine, choline, carnitine, trimethylamine (TMA), and TMA *N*-oxide concentrations were determined by a targeted metabolomics assay using liquid chromatography/mass spectrometry. Genomic DNA was isolated from whole-blood samples. DNAme was assessed using the Illumina Infinium Human Methylation EPIC BeadChip Array (EPIC 850K). Stool samples were self-collected by participants. DNA extracted from homogenized fecal isolates was analyzed for 16S rRNA genes. Additional details are in Supporting Information.

### Multiomic data analysis

A combined multiomic data set was created from baseline metabolites (number of features, $p = 5$), baseline GM ($p = 46$, retaining those genera with at least 15 of the 56 samples having relative abundance > 0.003 [10 reads]), and baseline DNAme ($p = 250$, retaining the 250 probes with the lowest $P$ values comparing baseline with 3 months). To capture the most robust responses in clinical outcomes, we calculated changes in clinical outcomes based on the earliest available timepoint (3 months for anthropometric measures, 6 months for body composition and blood chemistry). The multiomic data were combined with change data for 10 clinical outcomes for which there was a significant difference between baseline and the subsequent timepoint (weight, WC, FM, hemoglobin A$_{1c}$, homeostatic model assessment of insulin resistance, T. Chol, TG, CRP, leptin, ghrelin), excluding technical correlates of other measurements (BMI, glucose, and insulin). We fit a linear model to each pair of features spanning the assays (e.g., change in WC ~ baseline *Bifidobacterium*) (Figure 1B). To eliminate relationships potentially driven by outliers, we removed those models with a maximum standardized difference in fit value > 5 (76 models). We then created a network from the 25 models with the smallest slope $P$ values from each assay pair, subject to $P$ value < 0.05. Hereafter, we call this the multiomic network.

For each clinical outcome, we built a linear regression model containing all omic features in the network neighborhood of order 2, as well as potential confounders of age, sex, and the baseline value of the modeled outcome. Each model included only those participants for whom there was no missing data for the included predictors. We performed model selection using stepwise backward selection, with Akaike information criterion as the selection statistic. We allowed this process to eliminate both omic markers and potential confounders. To account for overfitting, we permuted outcome values 10,000 times and rederived both full and reduced models, calculating $P$ values as the fraction of times adjusted $R^2$ from the permuted model was greater than that from the observed data. Additional details are in Supporting Information. All analysis was performed in R version 3.5.1.
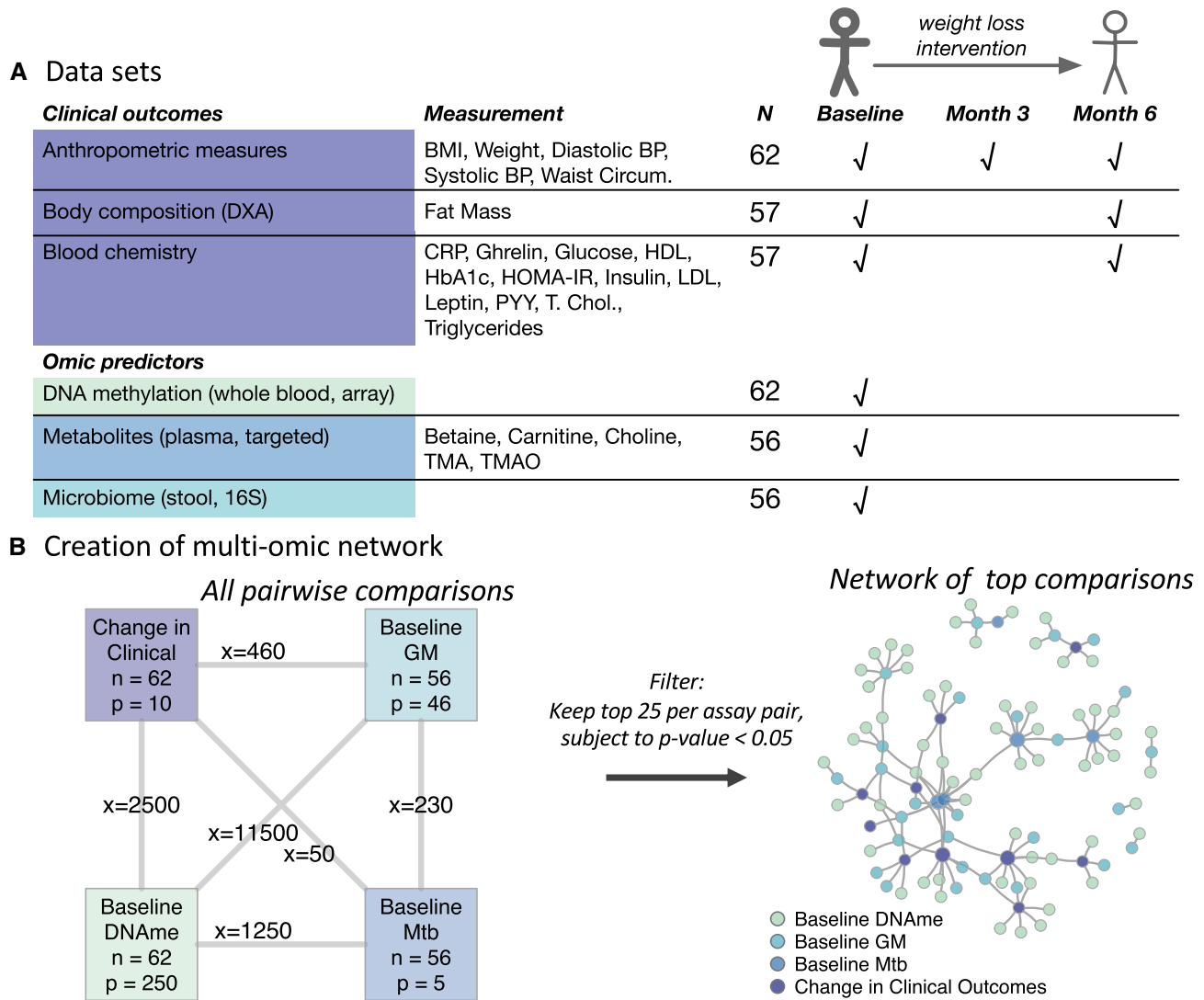
**Figure 1** Overview of data sets and network generation. (**A**) Participants were monitored for 6 months, with clinical outcomes assessed at baseline and at 3 and/or 6 months, depending on the outcome. Outcomes are grouped into anthropometric measures, body composition as measured by dual energy X-ray absorptiometry, and blood chemistry. Tissues drawn at baseline were interrogated by DNA methylation (DNAme) array, targeted metabolomics, and 16S rRNA sequencing assays. $N$ indicates the maximum number of participants with complete data for the analysis. For calculating change in clinical outcomes, data were required both at baseline and at 3 and/or 6 months. (**B**) Pairwise regression models were fit across four data categories (change in clinical outcome, baseline DNAme, baseline metabolites [Mtb], and baseline gut microbiome [GM]). The top 25 results per assay pair, based on smallest slope $P$ value subject to $P < 0.05$, were summarized in a multiomic network. The number of samples and number of features in each data category (e.g., $n = 56$ samples and $p = 250$ features for DNAme) are shown on the rectangles representing the categories. The number of pairwise comparisons across categories is indicated on the line connecting the categories. In the multiomic network, each node represents a feature, and each edge represents a regression between two features from different categories. The categories are color-coded according to the legend.

## Results

### Demographics and clinical outcomes

Characteristics of study participants are shown in Tables 1 and 2. Of the 62 participants, 75.8% were female, the mean age (SD) was 40.8 (9.7) years, and the mean baseline BMI was 33.2 (4.3) kg/m². Mean weight loss at month 3 was 5.9 (3.8) kg (range −15.9 to −0.4, $P = 3.6 \times 10^{-18}$) and at month 6 was 8.1 (5.8) kg. With the exception of SBP, diastolic blood pressure, low-density lipoprotein cholesterol, high-density lipoprotein cholesterol, and peptide YY, all clinical outcomes showed a statistically significant change at the analyzed timepoints (Table 2). The 6-month

values for weight, BMI, WC, and SBP are presented in Supporting Information Table S2. Of the 42 participants with complete diet diaries (7 days at baseline and 3 months), the mean percentage decrease from baseline in self-reported weekly energy intake was 27.9% (21.4%) (range −68.1% to 12.4%), equating to approximately 526 kcal/d.

### From data sets to a multiomic network

An overview of data sets and network generation is depicted in Figure 1. Participants were monitored for 6 months, with clinical outcomes assessed at baseline and again at 3 and/or 6 months, as shown in

**TABLE 1** Participant demographics

| Variable | Group | |
|---|---|---|
| *N* | | 62 |
| Age (mean ± SD) | | 40.8 ± 9.7 |
| | | |
| Sex (%) | Female | 47 (75.8) |
| | Male | 15 (24.2) |
| | | |
| Race: ethnicity (%) | Caucasian: Hispanic | 10 (16.1) |
| | Caucasian: non-Hispanic | 45 (72.6) |
| | Non-Caucasian: non-Hispanic | 7 (11.3) |

Figure 1A. Omic features were assessed at baseline. Sixty-two participants were selected for multiomic analysis. Of these, six did not consent to metabolomic analysis (remaining *n* = 56). Three did not submit stool samples, and another three stool samples were omitted because of low-quality sequencing (remaining *n* = 56). Figure 1B illustrates the steps in building the multiomic network: performing pairwise regressions across all omes, filtering results to retain the most promising, and summarizing these in a network. Each node represents a feature, and each edge a regression between two features from different omes.

## Visualizing crossomic relationships using VOLARE

A representative example of a subnetwork is shown in Figure 2A, which illustrates associations between change in TG levels and four gut microbial genera, three DNAme probes, and two metabolites. Figure 2B-2C shows detailed plots of the relationships between change in TG and baseline DNAme of a CpG, cg18366782, which is not annotated to any gene (Figure 2B), and baseline metabolite concentration of TMA (Figure 2C). The fitted regression lines show negative associations, representing larger reductions in TG in individuals who had higher baseline levels of DNAme of cg18366782 ($r = -0.46$, $P = 0.0004$) or TMA ($r = -0.32$, $P = 0.0199$). Visualizing these pairwise relationships in the VOLARE framework (12) allows us to vet the underlying data for magnitude and dynamic range, assess the relationship for goodness of fit, and borrow information from a feature in one ome to better understand a feature in another ome. For example, cg18366782 is not annotated to any particular gene yet is well correlated with change in TG levels.

## From network neighborhoods to predictive models

The overall network depicting the relationships between all clinical and omic features, first described in Figure 1B, is shown in greater detail in Figure 3A. Clinical outcome nodes are labeled, with the size of the node proportional to the size of its neighborhood of order 2 (the number of its neighbors and its neighbors' neighbors). Neighborhoods are shown for change in weight (Figure 3B), WC (Figure 3C), and TG (Figure 3D). In each of these neighborhoods, clinical outcomes are connected to features from each of the three omes. The neighborhoods range in size from 12 predictors for weight to 21 predictors for TG. All nonclinical nodes in the neighborhood were used as predictors in the model-building process. The nodes retained in the predictive models are larger than the nodes eliminated by backward selection.

**TABLE 2** Weight loss and clinical outcomes following a behavioral weight loss intervention

| | Baseline | 3 months | Change at 3 months | Change at 3 months, *P* value | *n* |
|---|---|---|---|---|---|
| Body weight (kg) | 95.3 ± 16.3 | 89.4 ± 15.3 | −5.9 ± 3.8 | **$3.6 \times 10^{-18}$** | 62 |
| BMI (kg/m²) | 33.2 ± 4.3 | 31.1 ± 4.1 | −2.1 ± 1.3 | **$1.2 \times 10^{-18}$** | 62 |
| Waist circumference (cm) | 108.4 ± 10.8 | 100.3 ± 10.7 | −8.1 ± 5.4 | **$2.7 \times 10^{-17}$** | 62 |
| Systolic BP (mmHg) | 117.7 ± 13.5 | 115.0 ± 11.3 | −2.9 ± 11.9 | $6.5 \times 10^{-2}$ | 61 |
| Diastolic BP (mmHg) | 74.6 ± 8.1 | 75.7 ± 9.0 | 1.0 ± 10.9 | $4.9 \times 10^{-1}$ | 61 |
| | Baseline | 6 months | Change at 6 months. | Change at 6 months, *P* value | *n* |
| Fat mass (kg) | 34.6 ± 8.3 | 29.0 ± 8.8 | −5.2 ± 3.8 | **$2.6 \times 10^{-14}$** | 57 |
| HbA$_{1c}$ (%) | 5.5 ± 0.3 | 5.4 ± 0.3 | −0.1 ± 0.2 | **$5.9 \times 10^{-3}$** | 57 |
| Glucose (mg/dL) | 93.0 ± 10.0 | 90.4 ± 7.6 | −2.6 ± 9.7 | **$4.5 \times 10^{-2}$** | 57 |
| Insulin (uIU/mL) | 11.1 ± 7.2 | 8.3 ± 5.9 | −3 ± 5 | **$3.8 \times 10^{-5}$** | 57 |
| HOMA-IR (mass units) | 2.6 ± 2 | 1.9 ± 1.4 | −0.8 ± 1.3 | **$3.9 \times 10^{-5}$** | 57 |
| T. Chol (mg/dL) | 187.0 ± 40.7 | 178.5 ± 36.2 | −10.4 ± 23 | **$1.3 \times 10^{-3}$** | 57 |
| Triglycerides (mg/dL) | 143.0 ± 87.1 | 111.4 ± 60.6 | −34.6 ± 63.9 | **$1.6 \times 10^{-4}$** | 57 |
| HDL (mg/dL) | 48.6 ± 12.6 | 49.6 ± 12.2 | 0.8 ± 6.7 | $4.1 \times 10^{-1}$ | 57 |
| LDL (mg/dL) | 109.4 ± 35.9 | 106.1 ± 30.1 | −4.3 ± 21 | $1.3 \times 10^{-1}$ | 57 |
| CRP (mg/L) | 5.0 ± 5.1 | 3.6 ± 4.5 | −1.5 ± 4 | **$8.0 \times 10^{-3}$** | 57 |
| Leptin (ng/nL) | 68.3 ± 43.8 | 35.9 ± 23.9 | −30.6 ± 33.3 | **$1.0 \times 10^{-8}$** | 55 |
| Ghrelin (pg/mL) | 902.8 ± 345.6 | 1,026.0 ± 425.5 | 124.6 ± 295.4 | **$2.6 \times 10^{-3}$** | 57 |
| PYY (pg/mL) | 92.7 ± 35.4 | 89.9 ± 26.6 | −2.4 ± 30.9 | $5.7 \times 10^{-1}$ | 57 |

Differences in parameters between baseline and subsequent time points were analyzed using paired *t* tests. Significance was set at $P < 0.05$ as indicated by bold *P* values. BP, blood pressure; HbA$_{1c}$, hemoglobin A$_{1c}$; HDL, high-density lipoprotein; HOMA- CRP, C-reactive protein; IR, homeostatic model assessment of insulin resistance; LDL, low-density lipoprotein; PYY: peptide YY; T. Chol, total cholesterol.
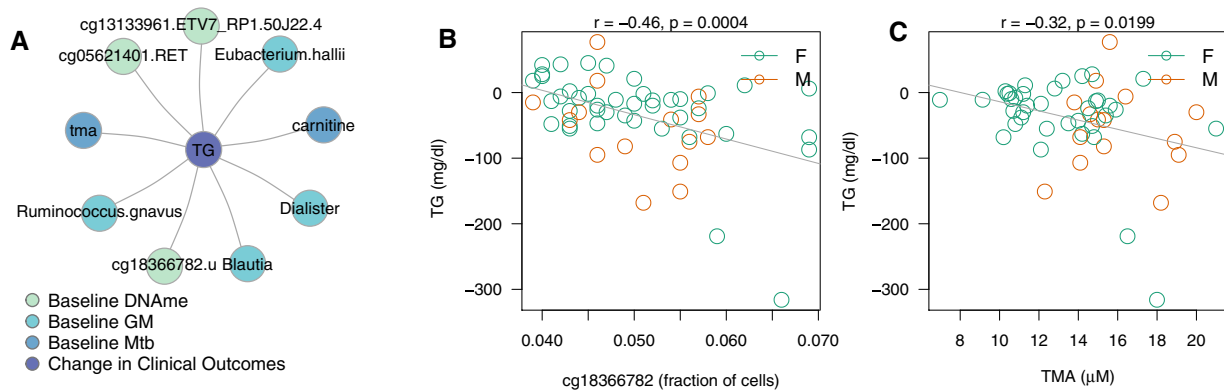
**Figure 2** Multiomic associations with change in triglycerides (TG). (**A**) Associations between change in TG and nine multiomic features: four gut microbial genera, three DNA methylation (DNAme) probes, and two metabolites. (**B**) A detailed plot showing the relationship between change in TG and baseline DNAme of a CpG site, cg18366782, which is unannotated. Each circle represents one study participant colored by sex (green = female, brown = male). The fitted regression line shows a negative association with larger reductions in TG corresponding to higher baseline levels of DNAme ($r = -0.46$, $P = 0.0004$). (**C**) Detailed plot for the relationship between change in TG and baseline concentration of metabolite trimethylamine (TMA). The fitted regression line shows a negative association with larger reductions in TG corresponding to higher levels of TMA ($r = -0.32$, $P = 0.0199$).

The reduced models for all 10 clinical outcomes included omic predictors, with the exception of FM. For FM, the reduced model consisted only of the mean value of FM, suggesting that we did not identify any good predictors. Of the remaining nine models, eight (weight, WC, homeostatic model assessment of insulin resistance, T. Chol, TG, CRP, leptin, and ghrelin) had adjusted $R^2$ values ranging from 0.34 to 0.78, and permutation $P$ values ranging from <0.0001 to 0.0118. Summary statistics for these reduced models are shown in Supporting Information Figure S1, with additional details in Supporting Information Table S1. Model details for weight, WC, and TG are presented below, with scatterplot matrices and pairwise correlation coefficients for the baseline values of the outcome, change in the outcome, and the omic predictors provided in Supporting Information Figures S2-S4.

## Predictive models for change in weight, WC, and TG

The predictive model for change in weight is shown in Figure 4 (adjusted $R^2 = 0.48$, permutation $P < 0.0001$). This model predicts change in weight using baseline levels of DNAme of a CpG site in the phosphofurin acidic cluster sorting 2 gene *(PACS2)* gene and four microbial genera. The relative importance of each predictor is expressed as an interquartile range (IQR) effect size (13). This represents the estimated change in response (e.g., weight) associated with a change in a predictor from the 25th percentile (first quartile) to the 75th percentile (third quartile), with all other predictors held constant. Increased methylation of cg25543749, ranging from 85.4% at the 25th percentile to 87.5% at the 75th percentile, was disadvantageous for weight loss, with an IQR effect size of 1.6 kg. This suggests that, all other factors being equal, a person with methylation of 85.4% is predicted to lose 1.6 kg more than a person with methylation of 87.5%. The converse is also true. *Coprococcus 3*, a microbe, was advantageous for weight loss, with an IQR effect size of −1.6 kg. In absolute terms, the largest effect sizes were ~ 25% of the mean change in weight.

The model for change in WC is illustrated in Figure 5 (adjusted $R^2 = 0.34$, permutation $P = 0.0118$). Baseline methylation of cg15869128 was advantageous for reduced WC, with an IQR of 2.25 cm. Increased baseline WC was also advantageous for reduced WC, with an IQR effect size of −1.6. In contrast, both *Bacteroides* and *Lachnospiraceae* were disadvantageous for reduced WC. In absolute terms, the largest effect sizes were ~ 27% to 30% of the mean change in WC.

The model for change in TG is shown in Figure 6 (adjusted $R^2 = 0.76$, permutation $P = 0.0003$). This was the most complex model, concordant with the size of the TG node (Figure 3A). Carnitine and TMA have effect sizes of similar magnitudes, though in opposite directions. High baseline TG levels were associated with a large decrease in TG, with an IQR effect size of −42 mg/dL. All but one of the remaining predictors showed effect sizes that, in absolute terms, were over 25% of the mean change in TG. Baseline relative abundance of the gut microbes *Faecalibacterium* and *Blautia* were associated with greater reductions in TG, with IQR effect sizes of −24 and −10, respectively. Male participants were predicted to have a 16 mg/dL disadvantage in reduction in TG, with all other factors held constant.

## Discussion

In this study, our goal was to identify baseline omic predictors of short-term weight loss and clinical outcomes during a behavioral-based weight loss intervention. Our results demonstrate that baseline multiomic features can provide important clinical insight at both the aggregate and individual participant level. Collectively, this work is a first step toward the development of precision nutrition approaches for weight loss and improved metabolic health, guided by baseline multiomic predictive models. The Diogenes study, a multicenter European dietary intervention, supported related work. Meyer et al. consider a binary predictor of changes in insulin sensitivity using clinical measurements and plasma metabolites and lipids (14). Ruffieux et al. present
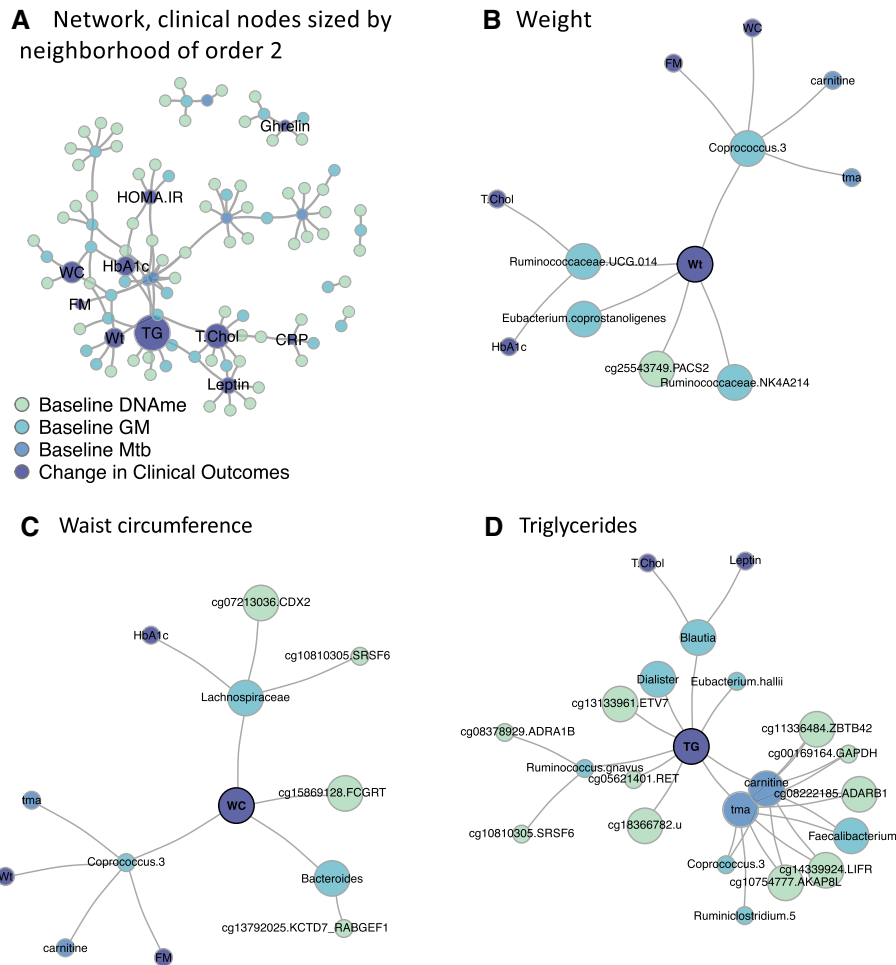
**Figure 3** Clinical neighborhoods of order 2. (**A**) The overall network with clinical outcomes labeled and sizes of the clinical nodes proportional to the size of their neighborhood of order 2. (**B-D**) Neighborhoods for change in weight, waist circumference (WC), and triglycerides (TG). Nodes retained in the predictive model after the model selection process are larger than the eliminated nodes. Color-coding as per panel A.

a computationally efficient approach to identify associations between SNPs and metabolites (15). Our work differs in that we consider three different omes and multiple continuous clinical outcomes.

## Change in weight

Participants lost, on average, 5.9 kg of weight from baseline to month 3, which is consistent with other behavioral weight loss programs (16). This degree of modest weight loss, even in the short term, has been shown to improve disorders associated with obesity, such as hypertension, dyslipidemia, and cardiovascular disease (17). However, the range of weight loss at 3 months (−15.9 to −0.4 kg) demonstrates wide interindividual variability. We identified five predictors of change in weight that included four gut microbes and one DNAme site.

Both *Ruminococcaeae NK4A214* and *Coprococcus 3* were advantageous for weight loss (Figure 4). *Ruminococcaeae NK4A214* was higher in people without obesity as compared with individuals with obesity (18). Higher *Coprococcus* was associated with reduced weight gain in mice fed a high-fat diet for 12 weeks (19). Protective effects

may be related to the ability of *Coprococcus* species to produce butyrate (20). Butyrate is a short-chain fatty acid (SCFA) resulting from gut microbial fermentation of dietary fiber that is well-known for its beneficial health effects and anti-inflammatory properties, and it acts as a histone deacetylase inhibitor, linking it to epigenetic effects (21).

Both *Ruminococcaceae UCG 014* and *Eubacterium coprostanoligenes* were disadvantageous for weight loss. *Ruminococcaea UCG 014* decreased with intermittent administration of a fasting-mimicking diet in mice (22). *Eubacterium coprostanoligenes* has been shown to convert cholesterol to coprostanol (23), an indicator of a cholesterol-rich diet (24). This may reflect that individuals with baseline high-cholesterol diets were less responsive to diet intervention, but further investigation is needed.

The DNAme site cg25543749 was also disadvantageous for weight loss, with a percentage change in methylation of 2.1 predictive of an ~1.6 kg change in weight. This site is located within intron 20 of the phosphofurin acidic cluster sorting 2 gene (*PACS2*), which is involved in metabolism and insulin signaling. Phosphorylation
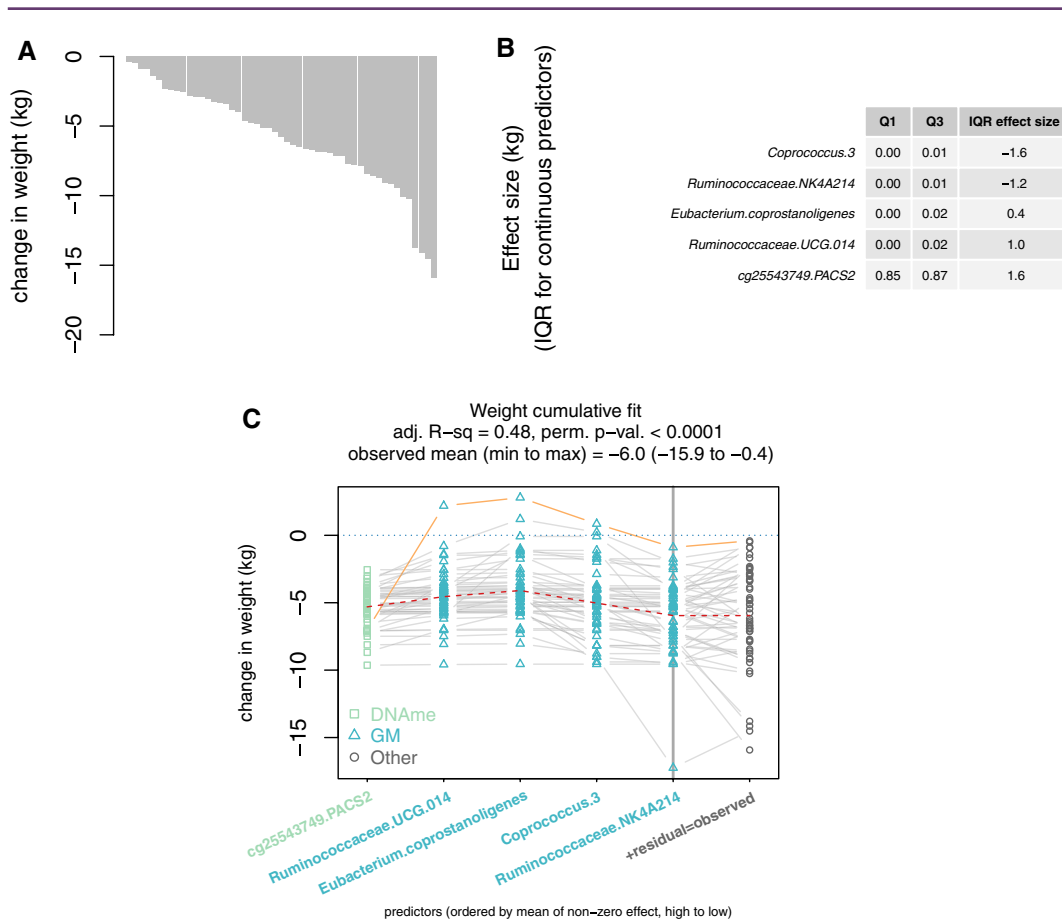
**Figure 4** Predictive model for change in weight at 3 months. (**A**) Waterfall plot illustrates variability in the change in weight, with each bar representing one study participant. (**B**) Interquartile range (IQR) effect sizes with predictors ordered by the effect size. The IQR effect size is the change in response associated with a change in a predictor from the first quartile (Q1, 25th percentile) to the third quartile (Q3, 75th percentile), which includes 50% of the data values. These effect sizes represent the relative importance of the predictors rather than shifts in the graph or the relative magnitude of predictors. (**C**) The cumulative fit graph displays estimated response (change in weight) by accumulating the contribution of one predictor at a time. Points represent the cumulative fit as various predictors are added to the total, with point shape and color representing the type of data. The gray line segments connect the points for each participant. To better illustrate the concept of the participant-level detail, the data for the participant with the highest level of *Ruminococcaceae. UCG.014* are shown in orange. The points on the gray vertical line toward the right side of the graph represent estimated response for each participant, whereas the right-most dark gray points indicate the observed responses. The dotted blue horizontal line at zero indicates no change in weight. A dotted red "trend line" connects the mean cumulative value at each predictor. The predictors are ordered by mean contribution to the fit, from highest to lowest. The intercept is not shown. DNAme, DNA methylation; GM, gut microbiome. [Color figure can be viewed at wileyonlinelibrary.com]

of *PACS2* has been associated with lipogenesis via mitochondrial-associated membrane interactions and inhibition of sirtuin 1 activity (25,26); sirtuin 1 is a NAD +-dependent histone deacetylase and is a key nutrient sensor responsive to fasting (27). Thus, *PACS2* is a biologically relevant gene target in the context of obesity, weight loss, and metabolism.

## Change in WC

Participants lost, on average, 8 cm of WC from baseline to month 3. Reductions in WC with weight loss are associated with greater improvements in components of the metabolic syndrome than changes in weight or BMI alone (28). The five predictors in the WC model (Figure 5) included two gut microbes, two DNAme sites, and baseline WC. *Bacteroides* and *Lachnospiraceae* were disadvantageous for

reductions in WC. Relative abundance of the genus *Bacteroides* has been associated with leanness in several studies (29), and *Bacteroides uniformis* protected against metabolic dysfunction in diet-induced obesity in mice (30). Bacteria in the family *Lachnospiraceae* that were undefined at the genus level had a large effect size in this model, but represent a heterogeneous group that is poorly defined functionally and may warrant further investigation at the sequence variant level.

One of the DNAme sites associated with reductions in WC was cg15869128, which is annotated to the first intron of the Fc fragment of IgG receptor and transporter (*FCGRT*) gene, a genomic location that is also a predicted promoter region for *FCGRT*. *FCGRT* is involved in passive immunity during early development and adaptive immunity
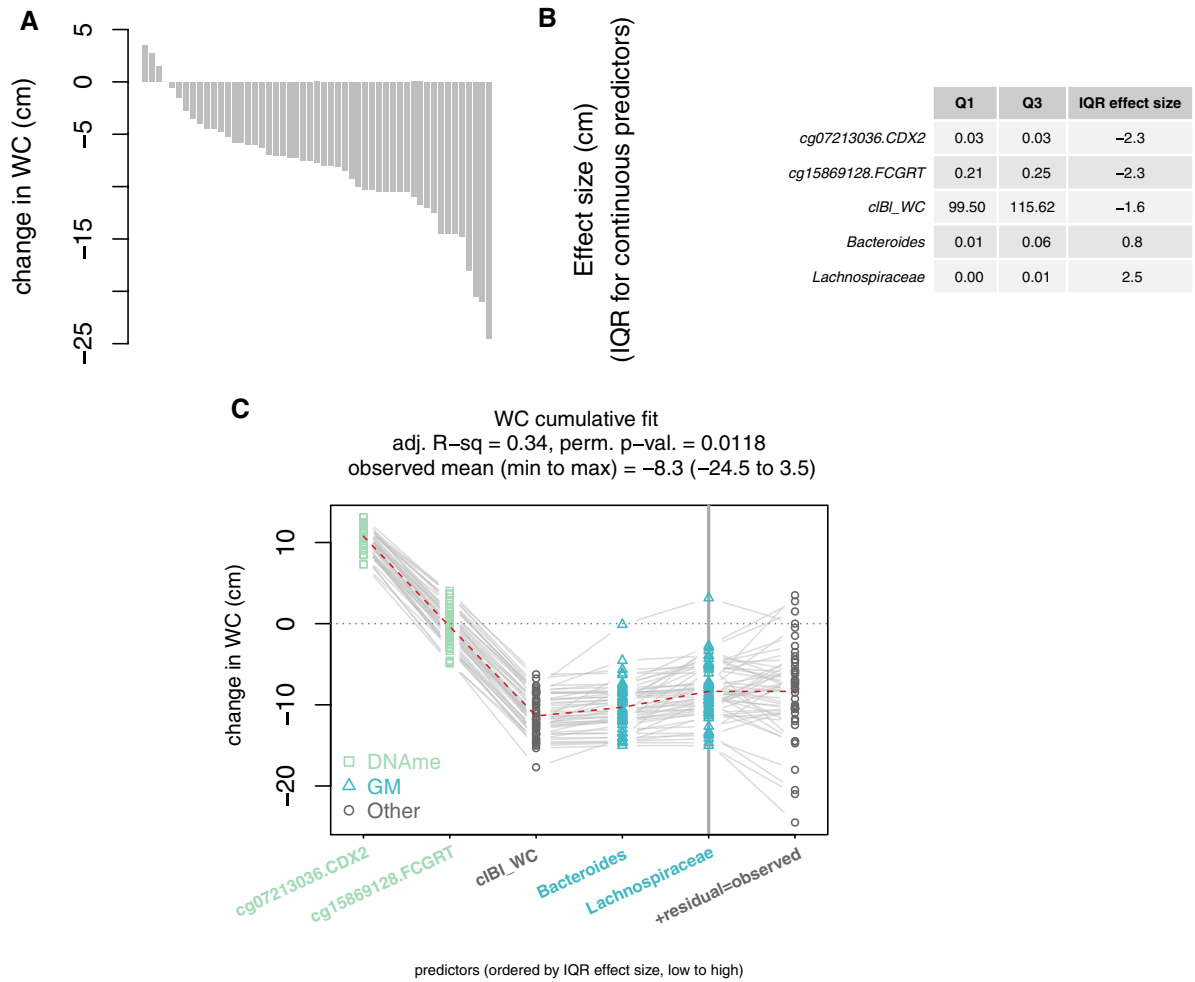
| | Q1 | Q3 | IQR effect size |
|---|---|---|---|
| *cg07213036.CDX2* | 0.03 | 0.03 | −2.3 |
| *cg15869128.FCGRT* | 0.21 | 0.25 | −2.3 |
| *clBI_WC* | 99.50 | 115.62 | −1.6 |
| *Bacteroides* | 0.01 | 0.06 | 0.8 |
| *Lachnospiraceae* | 0.00 | 0.01 | 2.5 |

**Figure 5** Predictive model for change in waist circumference at 3 months. (**A**) Waterfall plot illustrates variability in the change in waist circumference (WC), with each bar representing one study participant. (**B**) Interquartile range (IQR) effect sizes, with predictors ordered by the effect size. The IQR effect size is the change in response associated with a change in a predictor from the first quartile (Q1, 25th percentile) to the third quartile (Q3, 75th percentile), which includes 50% of the data values. (**C**) The cumulative fit graph displays estimated response (change in WC) by accumulating the contribution of one predictor at a time. Points represent the cumulative fit as various predictors are added to the total, with point shape and color representing the type of data. The gray line segments connect the points for each participant. The points on the gray vertical line toward the right side of the graph represent estimated response for each participant, whereas the right-most dark gray points indicate the observed responses. The dotted blue horizontal line at zero indicates no change in WC. A dotted red "trend line" connects the mean cumulative value at each predictor. The predictors are ordered by IQR effect size, low to high. The intercept is not shown. DNAme, DNA methylation; GM, gut microbiome. [Color figure can be viewed at wileyonlinelibrary.com]

throughout life (31). However, *FCGRT* has not been shown to be previously associated with WC, obesity, or weight loss. The DNAme site cg07213036 was also associated with reductions in WC. This site is annotated to the caudal type homeobox (*CDX2*) gene and located within a statistically significant differentially methylated region (Supporting Information Table S3), indicating that it was methylated in a similar manner as surrounding CpG sites. *CDX2* has been associated with WC and adiposity phenotypes (32) in a genetic variant of *CDX2*, rs11568820. Thus, *CDX2* methylation may warrant additional investigation.

## Change in TG

On average, TG decreased by 35 mg/dL over 6 months. The 13 predictors in the TG model (Figure 6) include three gut microbes, two metabolites, six DNAme sites, baseline TG levels, and sex. Among

blood lipids, TG has previously shown the strongest association with GM (33). *Faecalibacterium* and *Blautia* are associated with decreases in TG. The only described species in the *Faecalibacterium* genus is *F. prausnitzii*, one of the most abundant butyrate-producing species in the human gut (20). The *Blautia* genus has shown inconsistent relationships with cardiometabolic measures. Some studies have shown increased abundance with type 2 diabetes (34) and obesity (35), whereas another study has shown lower abundance with visceral fat (36). Although the effects of SCFA on metabolism are thought to be predominantly protective, increased levels of SCFA have been seen with obesity, which could represent an increased ability to harvest calories from food among individuals with obesity (37). In contrast, *Ruminococcus gnavus* was disadvantageous for reductions in TG. *R. gnavus* has been associated with obesity and metabolic disorders
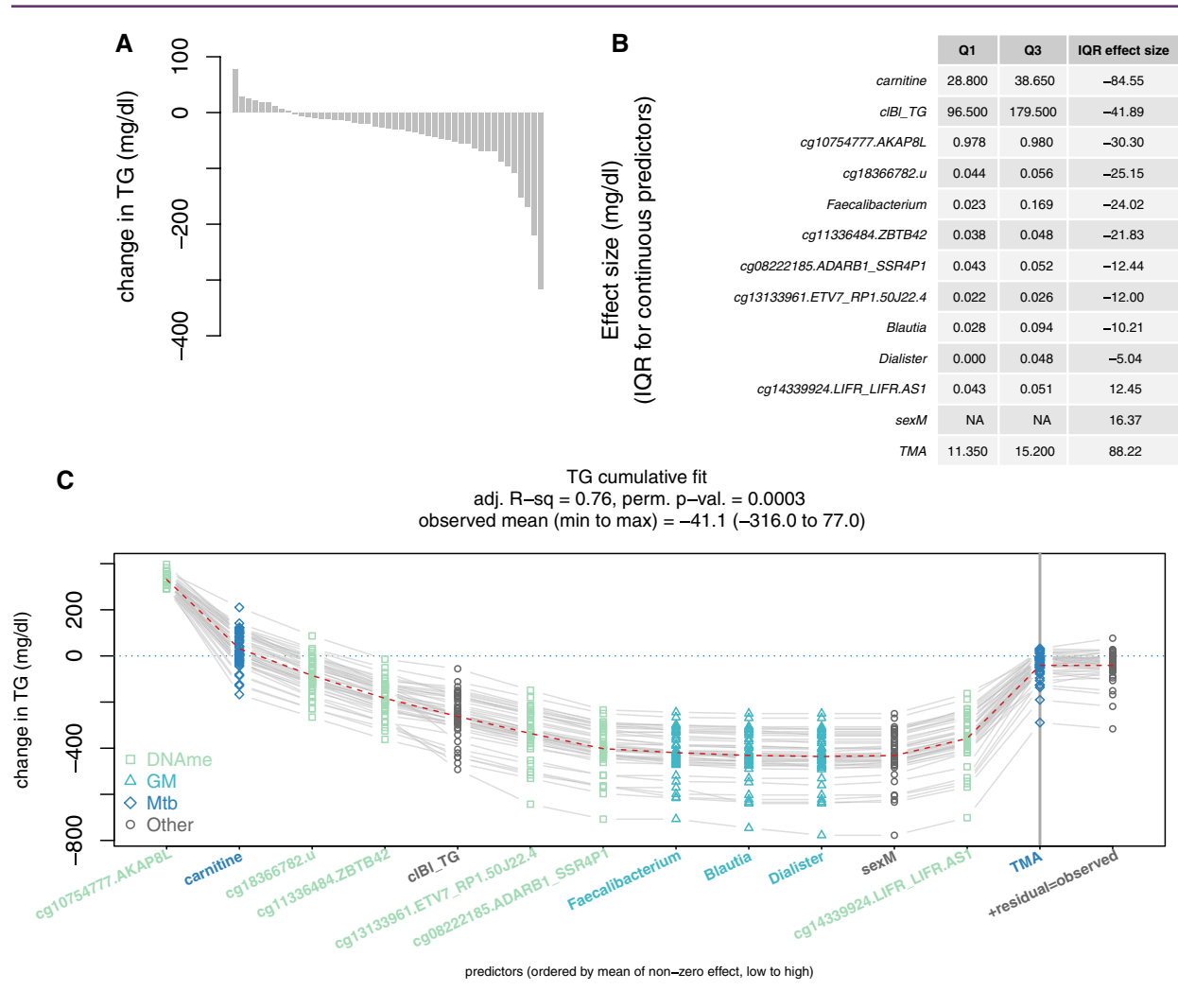
| | Q1 | Q3 | IQR effect size |
|---|---|---|---|
| *carnitine* | 28.800 | 38.650 | −84.55 |
| *clBI_TG* | 96.500 | 179.500 | −41.89 |
| *cg10754777.AKAP8L* | 0.978 | 0.980 | −30.30 |
| *cg18366782.u* | 0.044 | 0.056 | −25.15 |
| *Faecalibacterium* | 0.023 | 0.169 | −24.02 |
| *cg11336484.ZBTB42* | 0.038 | 0.048 | −21.83 |
| *cg08222185.ADARB1_SSR4P1* | 0.043 | 0.052 | −12.44 |
| *cg13133961.ETV7_RP1.50J22.4* | 0.022 | 0.026 | −12.00 |
| *Blautia* | 0.028 | 0.094 | −10.21 |
| *Dialister* | 0.000 | 0.048 | −5.04 |
| *cg14339924.LIFR_LIFR.AS1* | 0.043 | 0.051 | 12.45 |
| *sexM* | NA | NA | 16.37 |
| *TMA* | 11.350 | 15.200 | 88.22 |

**Figure 6** Predictive model for change in triglycerides (TG) at 6 months. (**A**) Waterfall plot illustrates variability in the change in TG, with each bar representing one study participant. (**B**) Interquartile range (IQR) effect sizes are shown below the graph, with predictors ordered by the effect size. The IQR effect size is the change in response associated with a change in a predictor from the first quartile (Q1, 25th percentile) to the third quartile (Q3, 75th percentile), which includes 50% of the data values. The effect size for sex is the difference in estimate for males. (**C**) The cumulative fit graph displays estimated response (change in TG) by accumulating the contribution of one predictor at a time. Points represent the cumulative fit as various predictors are added to the total, with point shape and color representing the type of data. The gray line segments connect the points for each participant. The points on the gray vertical line toward the right side of the graph represent estimated response for each person, whereas the right-most dark gray points indicate the observed responses. The dotted blue horizontal line at zero indicates no change in TG. A dotted red "trend line" connects the mean cumulative value at each predictor. The predictors are ordered by mean contribution to the fit, from lowest to highest. The intercept is not shown. DNAme, DNA methylation; GM, gut microbiome; Mtb, metabolite. [Color figure can be viewed at wileyonlinelibrary.com]

(38). It consumes mucins in the intestine and produces inflammatory polysaccharides (39), which could lead to intestinal dysbiosis that might exacerbate high TG.

Five of the six CpGs predictive of changes in TG are annotated to genes. Although cg18366782 is not proximal to any protein-coding genes, it was strongly associated with reductions in TG, which suggests that methylation of this CpG might warrant further investigation. Of the five remaining sites, four are annotated to genes that have not been previously associated with TG, weight loss, or obesity (Figure 6). Two sites, cg10754777 and cg11336484, are located in statistically significant differentially methylated regions (Supporting

Information Table S3). The DNAme site cg08222185 is annotated to the leukemia inhibitory factor receptor (*LIFR*) gene, a potential obesity drug treatment target (40), and is associated with lipogenic signaling in 3T3-L1 adipocytes (41). *LIFR* is known to heterodimerize with ciliary neurotrophic factor (*CNTF*), which may increase fatty acid oxidation and reduce insulin resistance in skeletal muscle via AMP-activated protein kinase activation (42).

The two metabolites in this model, carnitine and TMA, are highly correlated in our data (*r* = 0.99) and are indicated in Figure 3D by the preponderance of edges connecting microbes and DNAme probes to both carnitine and TMA. Carnitine, a nutrient abundant in red meat, is

metabolized by gut microbes into TMA, which is associated with cardiovascular disease (43). Although we did not perform any fine-tuning of our models, this correlation, coupled with the opposite directions of effects, suggests that one of these metabolites is a candidate for removal in a future model.

## Overall limitations

Despite salient and innovative qualities of the present study, there are limitations. The sample size was not adequate to capture the full diversity of the general population. The participants were primarily Caucasian females (64.5%), limiting generalizability. Although anthropometric measures were available at baseline and 3 months, blood chemistry was available at baseline and 6 months, per the protocol of the parent trial. Because the study is ongoing, we were blinded to intervention group assignment, which could be associated with additional variability in clinical outcomes that we were not able to model. We did not incorporate the role of dietary intake in our models. DNAme was measured in whole-blood samples rather than a metabolically active tissue like adipose, skeletal muscle, or liver. Whole blood is easier to obtain, thus facilitating measures at multiple time points. Furthermore, DNAme patterns in whole-blood can serve as a surrogate for those found in target tissues, such as adipose tissue (44). Because our long-term goal is to uncover modifiable predictors, we filtered DNAme to probes that were altered over time. Other filtering strategies were not investigated. Overall, our discussions of biological relevance are based on published literature and are associative in nature. However, the study has generated testable hypotheses for future experiments on metabolic targets and pathways.

## Overall strengths

By integrating omic data from biological systems known to interact and contribute to heterogeneity in clinical outcomes, we established the feasibility of using baseline omic features to predict clinical outcomes. These multiomic models are interpretable and parsimonious, at a level of detail that supports hypothesis generation and experimental follow-up. For example, *PACS2* gene and protein expression could be examined to further validate *PACS2* as a biomarker or test its role in a causal pathway. In addition, the identified predictors could be tested for association with longer-term weight loss (6 and 12 months) and weight loss maintenance (18 months). A possible approach is presented in Supporting Information Table S4. Both the models and the visualization thereof account for individual variability within and across predictors. An appreciation of this variability may inform the development of precision nutrition weight loss interventions. Furthermore, differences in predictors across clinical outcomes suggest that precision nutrition–based interventions might be tailored to specific clinical outcomes. For example, an intervention targeting shifts in the GM (e.g., consumption of foods rich in pre- and probiotics and dietary fiber) might be appropriate for someone who wants to reduce body mass (8,9,45), whereas a different intervention might be appropriate for someone who wants to reduce risk of cardiovascular disease (43).

In conclusion, using baseline omic predictors, we identified predictive models for changes in eight clinical outcomes during a weight loss intervention having adjusted $R^2$ values > 0.33. We provided in-depth discussion of biologically relevant predictors for weight, WC, and TG. Identification of baseline predictors of response is an initial step toward the development of personalized weight loss interventions. These findings provide a foundation for combating overweight and obesity by working with underlying biology rather than against it.**O**

## References

1. Flegal KM, Kruszon-Moran D, Carroll MD, Fryar CD, Ogden CL. Trends in obesity among adults in the United States, 2005 to 2014. *JAMA* 2016;315:2284-2291.
2. Centers for Disease Control and Prevention. Adult obesity facts. Reviewed February 11, 2021. Accessed July 31, 2020. https://www.cdc.gov/obesity/data/adult.html.
3. Ortega-Loubon C, Fernández-Molina M, Singh G, Correa R. Obesity and its cardiovascular effects. *Diabetes Metab Res Rev* 2019;35:e3135. doi:10.1002/dmrr.3135
4. Tobias DK, Chen M, Manson JE, Ludwig DS, Willett W, Hu FB. Effect of low-fat diet interventions versus other diet interventions on long-term weight change in adults: a systematic review and meta-analysis. *Lancet Diabetes Endocrinol* 2015;3:968-979. doi:10.1016/S2213-8587(15)00367-8
5. Johnston BC, Kanters S, Bandayrel K, et al. Comparison of weight loss among named diet programs in overweight and obese adults: a meta-analysis. *JAMA* 2014;312:923-933.
6. Herrmann SD, Willis EA, Honas JJ, Lee J, Washburn RA, Donnelly JE. Energy intake, nonexercise physical activity, and weight loss in responders and nonresponders: the Midwest Exercise Trial 2. *Obesity (Silver Spring)* 2015;23:1539-1549.
7. Zeisel SH. A conceptual framework for studying and investing in precision nutrition. *Front Genet* 2019;10:200. doi:10.3389/fgene.2019.00200
8. Ramos-Lopez O, Milagro FI, Allayee H, et al. Guide for current nutrigenetic, nutrigenomic, and nutriepigenetic approaches for precision nutrition involving the prevention and management of chronic diseases associated with obesity. *J Nutrigenet Nutrigenomics* 2017;10:43-62. doi: 10.1159/000477729
9. Zeisel SH. Precision (personalized) nutrition: understanding metabolic heterogeneity. *Annu Rev Food Sci Technol* 2020;11:71-92.
10. Aleksandrova K, Rodrigues CE, Floegel A, Ahrens W. Omics biomarkers in obesity: novel etiological insights and targets for precision prevention. *Curr Obes Rep* 2020;9:219-230.
11. Field AE, Camargo CA, Ogino S. The merits of subtyping obesity: one size does not fit all. *JAMA* 2013;310:2147-2148.
12. Siebert JC, Neff CP, Schneider JM, et al. VOLARE: Visual analysis of disease-associated microbiome-immune system interplay. *BMC Bioinformatics* 2019;20:432. doi:10.1186/s12859-019-3021-0
13. Harrell FE. *Regression Modeling Strategies: with Applications to Linear Models, Logistic Regression, and Survival Analysis*. New York: Springer; 2001.
14. Meyer A, Montastier E, Hager J, et al. Plasma metabolites and lipids predict insulin sensitivity improvement in obese, nondiabetic individuals after a 2-phase dietary intervention. *Am J Clin Nutr* 2018;108:13-23.
15. Ruffieux H, Davison AC, Hager J, Irincheeva I. Efficient inference for genetic association studies with multiple outcomes. *Biostatistics* 2017;18:618-636.
16. Franz MJ, VanWormer JJ, Crain AL, et al. Weight-loss outcomes: a systematic review and meta-analysis of weight-loss clinical trials with a minimum 1-year follow-up. *J Am Diet Assoc* 2007;107:1755-1767.
17. Goldstein DJ. Beneficial health effects of modest weight loss. *Int J Obes Relat Metab Disord* 1992;16:397-415.

18. Kellerer T, Brandl B, Büttner J, Lagkouvardos I, Hauner H, Skurk T. Impact of laparoscopic sleeve gastrectomy on gut permeability in morbidly obese subjects. *Obes Surg* 2019;29:2132-2143.

19. Wang Y, Tang C, Tang Y, Yin H, Liu X. Capsaicin has an anti-obesity effect through alterations in gut microbiota populations and short-chain fatty acid concentrations. *Food Nutr Res* 2020;64. doi:10.29219/fnr.v64.3525

20. Louis P, Flint HJ. Diversity, metabolism and microbial ecology of butyrate-producing bacteria from the human large intestine. *FEMS Microbiol Lett* 2009;294:1-8.

21. Chriett S, Dąbek A, Wojtala M, Vidal H, Balcerczyk A, Pirola L. Prominent action of butyrate over β-hydroxybutyrate as histone deacetylase inhibitor, transcriptional modulator and anti-inflammatory molecule. *Sci Rep* 2019;9:742. doi:10.1038/s41598-018-36941-9

22. Wei S, Han R, Zhao J, et al. Intermittent administration of a fasting-mimicking diet intervenes in diabetes progression, restores β cells and reconstructs gut microbiota in mice. *Nutr Metab* 2018;15:80. doi:10.1186/s12986-018-0318-3

23. Ren D, Li L, Schwabacher AW, Young JW, Beitz DC. Mechanism of cholesterol reduction to coprostanol by Eubacterium coprostanoligenes ATCC 51222. *Steroids* 1996;61:33-40.

24. Kübeck R, Bonet-Ripoll C, Hoffmann C, et al. Dietary fat and gut microbiota interactions determine diet-induced obesity in mice. *Mol Metab* 2016;5:1162-1174.

25. Krzysiak TC, Thomas L, Choi Y-J, et al. An insulin-responsive sensor in the SIRT1 disordered region binds DBC1 and PACS-2 to control enzyme activity. *Mol Cell* 2018;72:985-998. e7.

26. Thomas G, Aslan JE, Thomas L, Shinde P, Shinde U, Simmen T. Caught in the act - protein adaptation and the expanding roles of the PACS proteins in tissue homeostasis and disease. *J Cell Sci* 2017;130:1865-1876.

27. Nogueiras R, Habegger KM, Chaudhary N, et al. Sirtuin 1 and Sirtuin 3: physiological modulators of metabolism. *Physiol Rev* 2012;92:1479-1514.

28. Rothberg AE, McEwen LN, Kraftson AT, et al. Impact of weight loss on waist circumference and the components of the metabolic syndrome. *BMJ Open Diabetes Res Care* 2017;5:e000341. doi:10.1136/bmjdrc-2016-000341

29. Castaner O, Goday A, Park Y-M, et al. The gut microbiome profile in obesity: a systematic review. *Int J Endocrinol* 2018;2018:4095789. doi:10.1155/2018/4095789

30. Gauffin Cano P, Santacruz A, Moya Á, Sanz Y. Bacteroides uniformis CECT 7771 ameliorates metabolic and immunological dysfunction in mice with high-fat-diet induced obesity. *PLoS One* 2012;7:e41079. doi:10.1371/journal.pone.0041079

31. Kuo TT, Baker K, Yoshida M, et al. Neonatal Fc receptor: from immunity to therapeutics. *J Clin Immunol* 2010;30:777-789.

32. Ochs-Balcom HM, Chennamaneni R, Millen AE, et al. Vitamin D receptor gene polymorphisms are associated with adiposity phenotypes. *Am J Clin Nutr* 2011;93:5-10.

33. Fu J, Bonder MJ, Cenit MC, et al. The gut microbiome contributes to a substantial proportion of the variation in blood lipids. *Circ Res* 2015;117:817-824.

34. Egshatyan L, Kashtanova D, Popenko A, et al. Gut microbiota and diet in patients with different glucose tolerance. *Endocr Connect* 2016;5:1-9.

35. Kasai C, Sugimoto K, Moritani I, et al. Comparison of the gut microbiota composition between obese and non-obese individuals in a Japanese population, as analyzed by terminal restriction fragment length polymorphism and next-generation sequencing. *BMC Gastroenterol* 2015;15:100. doi:10.1186/s12876-015-0330-2

36. Ozato N, Saito S, Yamaguchi T, et al. Blautia genus associated with visceral fat accumulation in adults 20-76 years of age. *NPJ Biofilms Microbiomes* 2019;5:28. doi:10.1038/s41522-019-0101-x

37. Turnbaugh PJ, Ley RE, Mahowald MA, Magrini V, Mardis ER, Gordon JI. An obesity-associated gut microbiome with increased capacity for energy harvest. *Nature* 2006;444:1027-1031.

38. Le Chatelier E, Nielsen T, Qin J, et al. Richness of human gut microbiome correlates with metabolic markers. *Nature* 2013;500:541-546.

39. Henke MT, Kenny DJ, Cassilly CD, Vlamakis H, Xavier RJ, Clardy J. Ruminococcus gnavus, a member of the human gut microbiome associated with Crohn's disease, produces an inflammatory polysaccharide. *Proc Natl Acad Sci U S A* 2019;116:12672-12677.

40. Ortega FJ, Mercader JM, Catalán V, et al. Targeting the circulating MicroRNA signature of obesity. *Clin Chem* 2013;59:781-792.

41. Hogan JC, Stephens JM. Effects of leukemia inhibitory factor on 3T3-L1 adipocytes. *J Endocrinol* 2005;185:485-496.

42. Watt MJ, Dzamko N, Thomas WG, et al. CNTF reverses obesity-induced insulin resistance by activating skeletal muscle AMPK. *Nat Med* 2006;12:541-548.

43. Tang WHW, Li DY, Hazen SL. Dietary metabolism, the gut microbiome, and heart failure. *Nat Rev Cardiol* 2019;16:137-154.

44. Huang Y-T, Chu SU, Loucks EB, et al. Epigenome-wide profiling of DNA methylation in paired samples of adipose tissue and blood. *Epigenetics* 2016;11:227-236.

45. Zmora N, Suez J, Elinav E. You are what you eat: Diet, health and the gut microbiota. *Nat Rev Gastroenterol Hepatol* 2019;16:35-56.